Supplemental Figures

Supplemental Figure 1.

Comparison of D156844 binding to human DcpS in the closed conformation vs. the binding of m7GpppA to human eIF4E (PDB ID: 1IPB).

The LSQ function of the software program COOT [1] was used to superimpose the structure of m7G portion of m7GpppA (labeled stick) bound to human eIF4E (grey residues) in PDB ID:1IPB [2] to the m7G portion of the m7GpppG in the closed active site conformation of human DcpS in PDB ID:1ST0) [3]. This effectively aligned the eIF4E cap binding pocket with that of the closed active site of DcpS. The SSM function of COOT was then used to superpose the structure of D156844 (stick) bound in the closed active site conformation of DcpS (red residues) onto the structure of human DcpS with m7GpppG bound (PDB ID:1ST0). This operation effectively achieved the superposition of the D156844 conformation in the closed active site of DcpS (green stick) to that of m7GpppA bound to eIF4E. Residues are numbered and labeled accordingly.

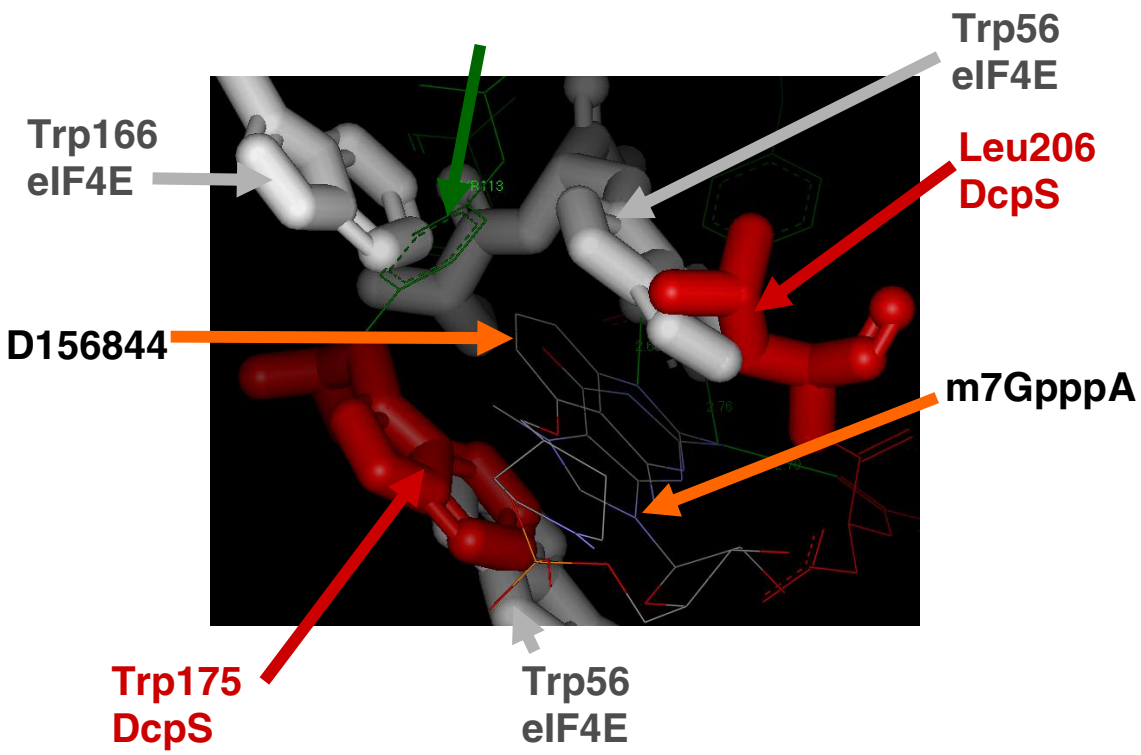

Supplemental Figure 2.

Comparison of D156844 binding to human DcpS in the closed conformation vs. the binding of m7GpppA to human eIF4E (PDB ID: 1IPB) shown together with a computationally docked D156844 into eIF4E.

The LSQ function of the software program COOT [1] was used to superimpose the structure of m7G portion of m7GpppA (labeled atom colored line structure) bound to human eIF4E (cyan residues) in PDB ID:1IPB [2] to the m7G portion of the m7GpppG in the closed active site conformation of human DcpS in PDB ID:1ST0) [3]. This effectively aligned the eIF4E cap binding pocket with that of the closed active site of DcpS. The SSM function of COOT was then used to superpose the structure of D156844 (green stick) bound in the closed active site conformation of DcpS onto the structure of human DcpS with m7GpppG bound (PDB ID:1ST0). This operation effectively achieved the superposition of the D156844 conformation in the closed active site of DcpS (green stick) to that of m7GpppA bound to eIF4E (labeled atom colored line structure). In addition, computational docking studies were carried out to arrive at a docked pose of D156884 in eIF4E (grey stick).

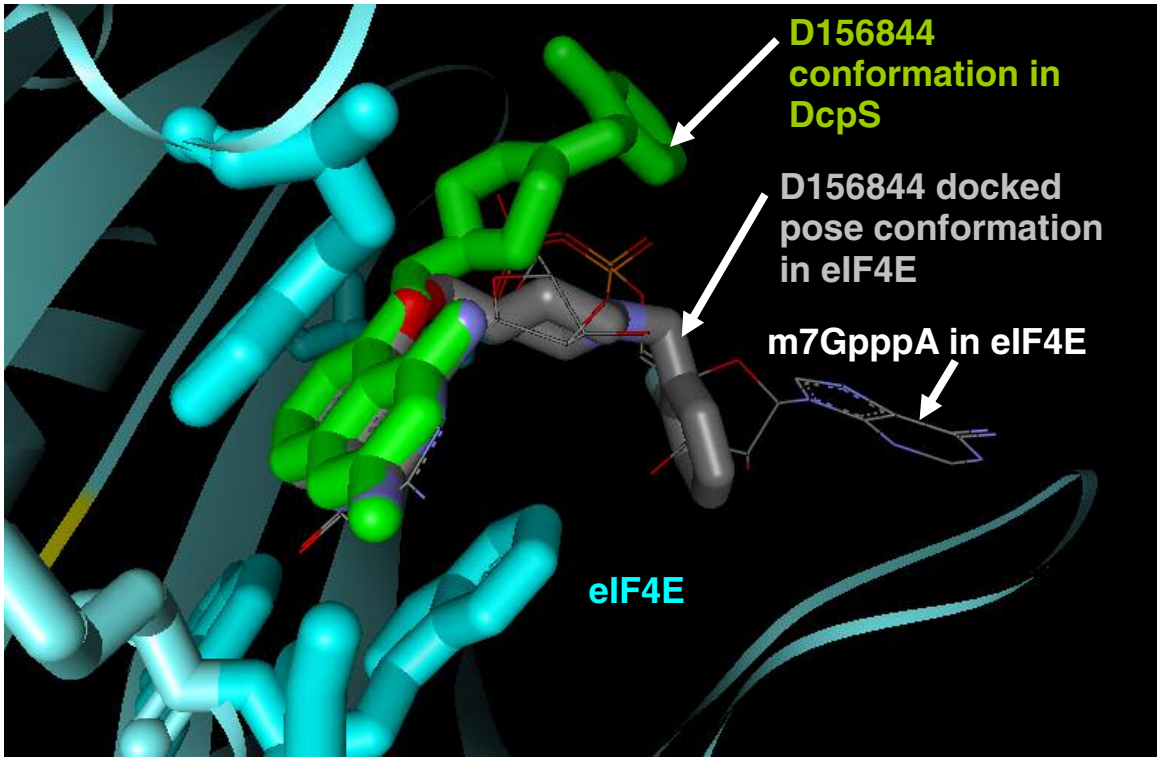

Supplemental Figure 3.

Comparison of D156844 binding to human DcpS in the closed conformation vs. the binding of m7GpppG to human p20 (PDB ID: 1N52) shown together with a computationally docked D156844 into p20.

The LSQ function of the software program COOT [1] was used to superimpose the structure of m7G portion of m7GpppG (labeled atom colored line structure) bound to human p20 subunit of Cap Binding Complex (cyan residues) in (PDB ID:1N52) [4] to the m7G portion of the m7GpppG in the closed active site conformation of human DcpS in PDB ID:1ST0) [3]. This effectively aligned the p20 cap binding pocket with that of the closed active site of DcpS. The SSM function of COOT was then used to superpose the structure of D156844 (green stick) bound in the closed active site conformation of DcpS onto the structure of human DcpS with m7GpppG bound (PDB ID:1ST0). This operation effectively achieved the superposition of the D156844 conformation in the closed active site of DcpS to that of m7GpppG bound to p20. In addition, computational docking studies with p20 were carried out to arrive at a docked pose of D156884 in p20 (grey stick).

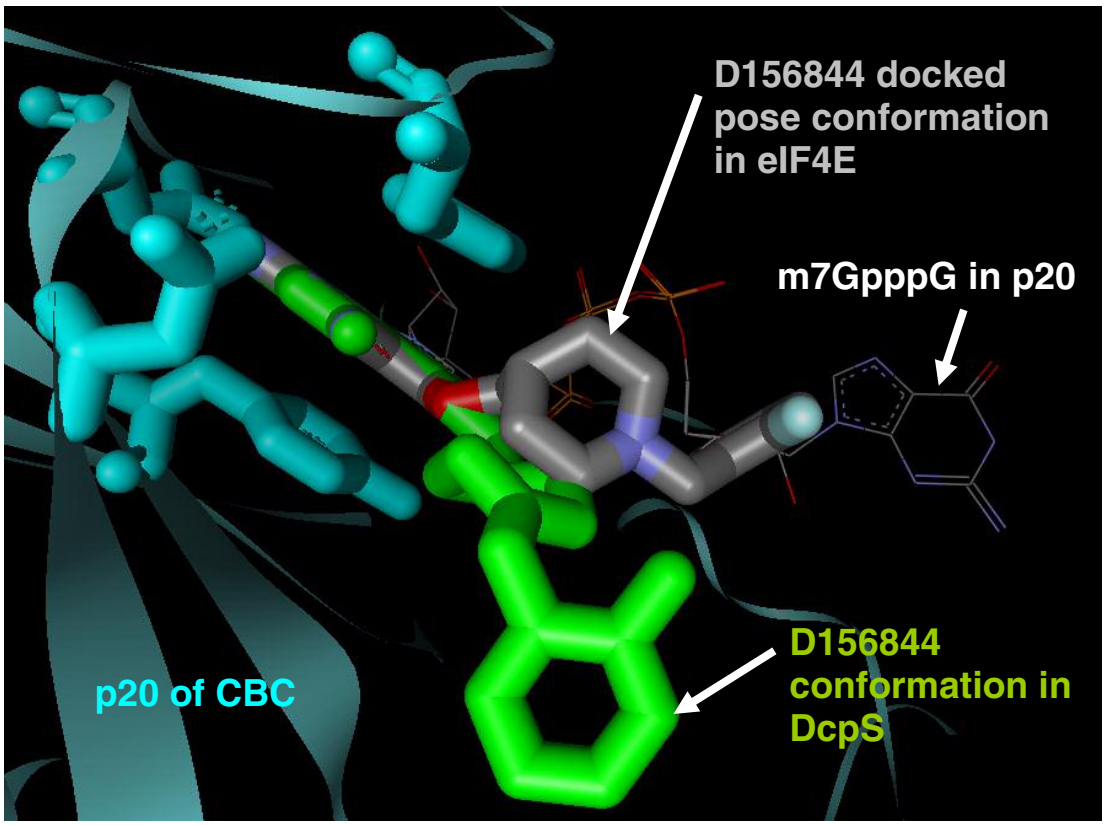

Supplementary Figure 4

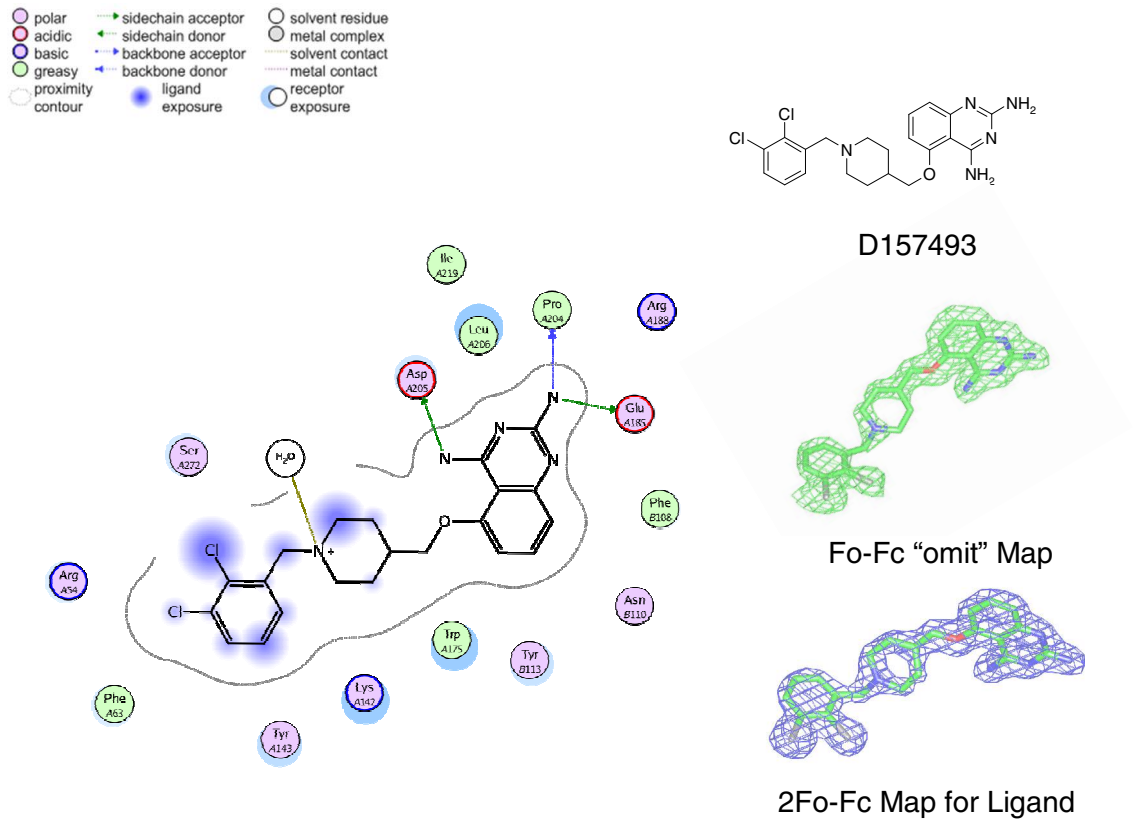

Ligand Interaction Figure of D157493 bound to Human DcpS "Closed" Active Site

Left Panel. DcpS amino acid interactions with D157493 are depicted schematically for the closed active site. The "A" and "B" subunit residues are listed with "*A*" or "*B*" prefixing the residue number. The figure was generated by the MOE software package (Chemical Computing Group, Montreal, Canada), with legend shown. *Upper Right Panel.* The chemical structure of D157493. *Middle Right Panel.* Green wire, 3.0 sigma positive electron density(|Fo|-|Fc|) of omit map of D157493 bound in the closed active site of human DcpS. *Lower Right Panel.* Blue wire, final 2|Fo|-|Fc| electron density map of D157493 bound in the closed active site of human DcpS.

Supplemental Figure 5.

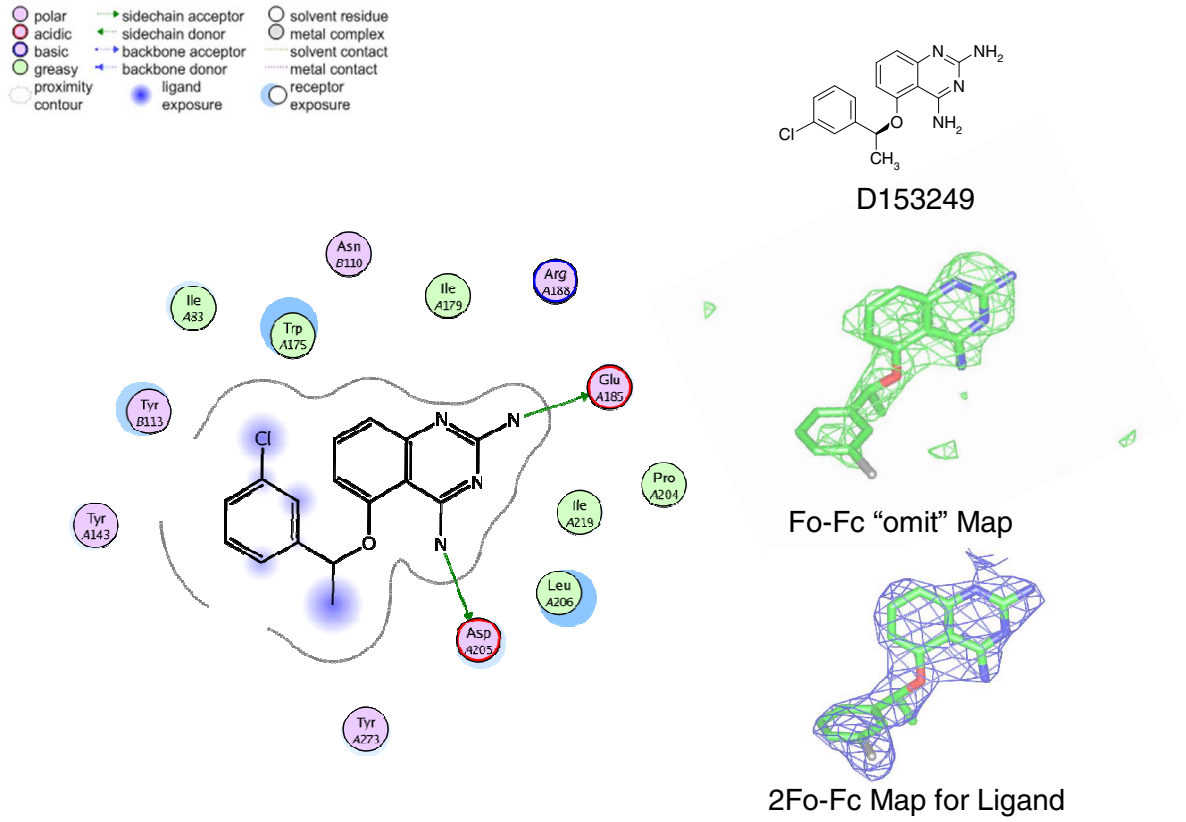

Ligand Interaction Figure of D153249 bound to Human DcpS "Closed" Active Site

Left Panel. DcpS amino acid interactions with D153249 are depicted schematically for the closed active site. The "A" and "B" subunit residues are listed with "*A*" or "*B*" prefixing the residue number. The figure was generated by the MOE software package (Chemical Computing Group, Montreal, Canada), with legend shown. *Upper Right Panel.* The chemical structure of D153249. *Middle Right Panel.* Green wire, 3.0 sigma positive electron density(|Fo|-|Fc|) of omit map of D157493 bound in the closed active site of human DcpS. *Lower Right Panel.* Blue wire, final 2|Fo|-|Fc| electron density map of D153249 bound in the closed active site of human DcpS.

Supplemental Figure 6.

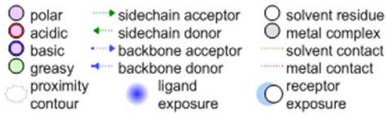

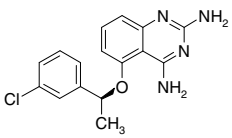

D153249

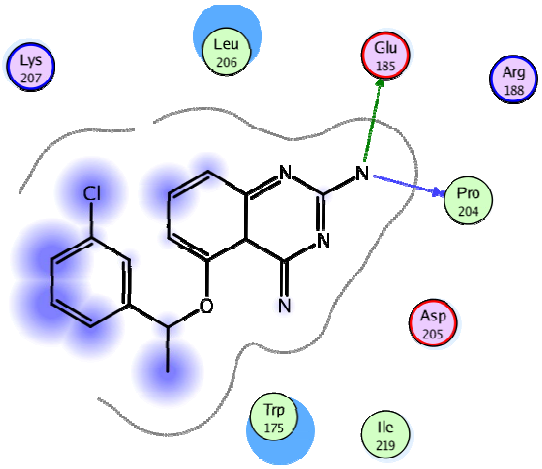

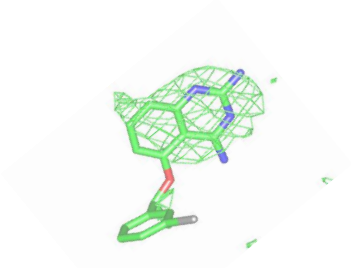

Fo-Fc "omit" Map

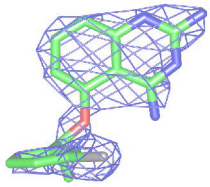

2Fo-Fc Map for Ligand

Ligand Interaction Figure of D153249 bound to Human DcpS "Open" Active Site

Left Panel. DcpS amino acid interactions with D153249 are depicted schematically for the open active site. The "A" and "B" subunit residues are listed with "*A*" or "*B*" prefixing the residue number. The figure was generated by the MOE software package (Chemical Computing Group, Montreal, Canada), with legend shown. *Upper Right Panel.* The chemical structure of D153249. *Middle Right Panel.* Green wire, 3.0 sigma positive electron density(|Fo|-|Fc|) of omit map of D157493 bound in the open active site of human DcpS. *Lower Right Panel.* Blue wire, final 2|Fo|-|Fc| electron density map of D153249 bound in the open active site of human DcpS.

Supplementary Table 1. Codon usage frequency table for highly expressed E. coli protein open reading frames. Shaded codons fall below the 2% frequency cutoff and were are not used during the synthetic gene sequence design of Δ37hDcpS by the Gene Composer™. The available (unshaded) codons were built into the synthetic gene for Δ37hDcpS at re-normalized frequencies.

Cdn	AmAcid	Freq	Cdn	AmAcid	Freq	Cdn	AmAcid	Freq	Cdn	AmAcid	Freq
Ala	GCA	0.28	Gln	CAA	0.14	Leu	CTT	0.05	Ser	TCG	0.04
Ala	GCC	0.07	Gln	CAG	0.86	Leu	TTA	0.03	Ser	TCT	0.39
Ala	GCG	0.21	Glu	GAA	0.83	Leu	TTG	0.02	Stop	TAA	0.83
Ala	GCT	0.45	Glu	GAG	0.17	Lys	AAA	0.81	Stop	TAG	0.17
Arg	AGA	0.02	Gly	GGA	0	Lys	AAG	0.19	Stop	TGA	0
Arg	AGG	0	Gly	GGC	0.5	Met	ATG	1	Thr	ACA	0.02
Arg	CGA	0	Gly	GGG	0.01	Phe	TTC	0.79	Thr	ACC	0.56
Arg	CGC	0.24	Gly	GGT	0.48	Phe	TTT	0.21	Thr	ACG	0.05
Arg	CGG	0.01	His	CAC	0.83	Pro	CCA	0.08	Thr	ACT	0.36
Arg	CGT	0.73	His	CAT	0.17	Pro	CCC	0.01	Trp	TGG	1
Asn	AAC	0.91	Ile	ATA	0.02	Pro	CCG	0.82	Tyr	TAC	0.8
Asn	AAT	0.09	Ile	ATC	0.86	Pro	CCT	0.08	Tyr	TAT	0.2
Asp	GAC	0.72	Ile	ATT	0.12	Ser	AGC	0.15	Val	GTA	0.21
Asp	GAT	0.28	Leu	CTA	0.01	Ser	AGT	0.01	Val	GTC	0.07
Cys	TGC	0.8	Leu	CTC	0.06	Ser	TCA	0.02	Val	GTG	0.15
Cys	TGT	0.2	Leu	CTG	0.83	Ser	TCC	0.39	Val	GTT	0.57

1. Emsley, P.; Cowtan, K., Coot: Model-Building Tools for Molecular Graphics. *Acta Cryst* **2004,** D60, 2126-2132.
2. Tomoo, K.; Shen, X.; Okabe, K.; Nozoe, Y.; Fukuhara, S.; Morino, S.; Ishida, T.; Taniguchi, T.; Hasegawa, H.; Terashima, A.; Sasaki, M.; Katsuya, Y.; Kitamura, K.; Miyoshi, H.; Ishikawa, M.; Miura, K., Crystal structures of 7-methylguanosine 5'-triphosphate (m(7)GTP)- and P(1)-7-methylguanosine-P(3)-adenosine-5',5'-triphosphate (m(7)GpppA)-bound human full-length eukaryotic initiation factor 4E: biological importance of the C-terminal flexible region. *Biochem J* **2002,** 362, (Pt 3), 539-44.
3. Gu, M.; Fabrega, C.; Liu, S. W.; Liu, H.; Kiledjian, M.; Lima, C. D., Insights into the structure, mechanism, and regulation of scavenger mRNA decapping activity. *Mol Cell* **2004,** 14, (1), 67-80.
4. Calero, G.; Wilson, K. F.; Ly, T.; Rios-Steiner, J. L.; Clardy, J. C.; Cerione, R. A., Structural basis of m7GpppG binding to the nuclear cap-binding protein complex. *Nat Struct Biol* **2002,** 9, (12), 912-7.